Proceedings of 14th IOE Graduate Conference
Peer Reviewed
Year: 2023 Month: December Volume: 14
ISSN: 2350-8914 (Online), 2350-8906 (Print)

Design and Analysis of Wing-Fuselage Attachment Lug of a General Aviation Aircraft

Bharat Kumar Budha Chhetri [a], Sunil Adhikari [b]

[a, b] *Department of Automobile and Mechanical Engineering, Thapathali Campus IOE, Tribhuvan University, Nepal*
[a] chhetribharat08@gmail.com, [b] suniladhikari144@gmail.com

Abstract
The objective of the study is to design wing-fuselage attachment lug and then perform the stress analysis of wing-fuselage attachment lug. The Computer-Aided Design (CAD) models of wing-fuselage attachment lug was developed using the Computer Aided Three-Dimensional Interactive Application (CATIA) V5 software. The different model of wing-fuselage attachment lug varying lug thickness and number of bolt holes are analyzed based on combined steel alloy AISI 4340 and Aluminum 2024-T351 materials and AISI 4340 materials only. The results showed that the wing-fuselage attachment with aluminum spar attached with the designed lug do not satisfy the strength requirement. The wing-fuselage attachment using AISI 4340 materials only satisfies the strength requirement and hence is safe structure for the studied general aviation aircraft.

Keywords
Aircraft Design, Structural Analysis, Lug, Single-Engine Aircraft

1. Introduction

Lugs are important and critical connector type elements widely used as structural supports for connections in aircraft structure. One typical applications of lug is attaching wing to the fuselage attachment of an airplane. Different types of loads are subjected to airplane wings so it is essential to be rigidly fix the wing to the fuselage. This attachment is done by required number of lugs between the wing side of wing box and the fuselage through which the loads are transferred from wing to fuselage thus, aircraft wing fuselage attachment lug is the one on which the maximum loads act [1, 2]. Loss of load carrying capacity of lug joints could lead to the catastrophic failure of the whole structure. [3, 4]. Designer performs finite element analysis studies and experimental studies to ensure the structure won't fail catastrophically. Attachment lugs are critical components where chances of fatigue growth are higher. The consequences can be severe due to possibility for the wing and fuselage to separate and results in accidents. Therefore, it is crucial to ensure aircraft attachment lug's damage tolerance by establishing design criteria and analysis methods.

[5] performed stress analysis on wing–fuselage attachment bracket of six-seater aircraft and the maximum tensile stress was observed 1373 N/mm^2 at one of the rivet hole of I-section spar. [6] studied the wing–fuselage joint analysis considering different materials. This work reported that aluminium-based materials are more suitable for the component. [7] conducted the stress analysis on transport aircraft wing–fuselage lug attachment bracket and reported the maximum tensile stress and displacement of a lug joint [8] performed simulation analysis over a fuselage and fuselage wing attachment bracket. The result showed the maximum tensile stress occurring location and quantity over an aircraft structure. [9] studied wing lug bracket assembly. This paper revealed that different methods of optimization and upgraded models used reduced stress and displacement as compared to existing methods.

The main objective of the present paper is to design and study various spar and wing fuselage attachment lug models in terms of stress analysis for a wing fuselage attachment of a conceptually designed general aviation aircraft using finite element software package Abaqus.

2. The Conceptual Design

2.1 Design Requirements

Conceptual design began with defining a set of design goals based on data collected for multiple aircraft within the same category. The operational parameters goals for single engine aircraft are as follows: Maximum speed greater than 71 m/s, stall speed greater than 23 m/s, takeoff run less than 500 m, landing distance less than 507 m, range of 400 nautical mile, service ceiling of 13120 ft and a maximum rate of climb of 4.2 m/s [10].

2.2 Mission profile and initial sketch

For the sake of this design analysis, a straight forward mission profile with six segments—takeoff, climb, cruise, descent, loiter, and landing—is taken into consideration and is depicted in Figure 1.

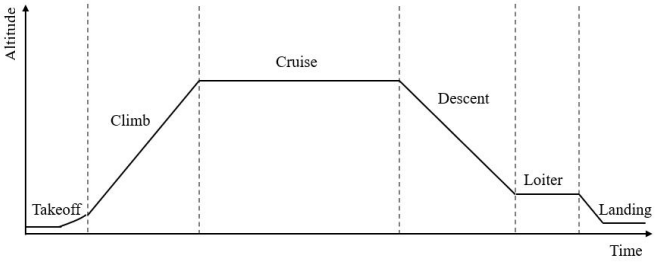

Figure 1: Mission Profile

The initial sketch of the aircraft is shown in Figure 2.

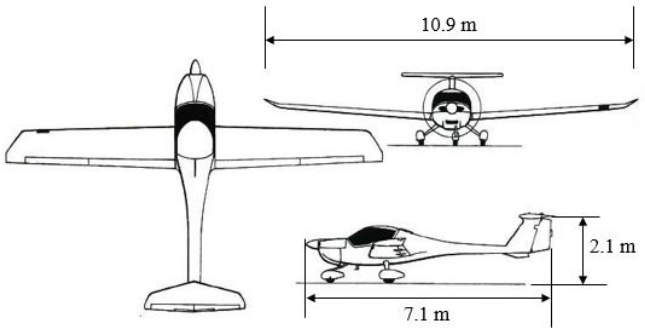

Figure 2: Initial Sketch[11]

2.3 Estimation of aircraft weight from initial sketch

There are four components to an airplane's gross takeoff weight: crew, payload, fuel, and empty weight. The design goals provide the crew and payload weights. The weight estimating procedure is iterative and is based on an initial estimate of the gross takeoff weight because the fuel and empty weight are unknown and depend on the takeoff gross. The gross takeoff weight is estimated using Equation (1) [12].

$$W_o = W_c + W_p + W_f + W_e \tag{1}$$

The take-off gross weight is stated in terms of the crew and payload weight, the fuel weight fraction, and the empty weight fraction as the elements in the above equation are rearranged. [12]

$$W_o = \frac{W_c + W_p}{1 - \left(W_f / W_o\right) - \left(W_e / W_o\right)} \tag{2}$$

Based on statistical data, the empty weight fraction can be expressed as follows [12].

$$\frac{W_e}{W_o} = A W_o^C \tag{3}$$

The statistical constants A and C in the equation above depend on the family of the aircraft as well as its shape, which is speculatively depicted in the Figure 2 sketch. Parameters A and C have values of 2.36 and -0.18, respectively [12]. However, the mission profile segments are used to calculate the fuel weight fraction; each segment uses a certain amount of fuel, and the total fuel weight fraction is the multiple of these fractions. This approach yields an approximate gross weight estimate of 820 kg for the aircraft. [12, 13] contains further information regarding the computation of the fuel weight fraction and the empty weight fraction.

2.4 Geometry sizing

The weight estimated in Section 2.3 can now be used to determine the geometry of the aeroplane wing. Through the computation of the airplane's weight and wing loading, the planform area of the wing (S) is determined to be 9.9 m^2. Based on an aspect ratio of 10 [13], the span is estimated to be 9.94 m. With a taper ratio which is the ratio between the tip and the root cords of 0.45,the root and tip cord values are 1.37 m and 0.62 m, respectively. Mean aerodynamic cord is located at 1.04 m from the root with a length of 2.17 m. An outline of the wings reference area is presented in Figure 3.

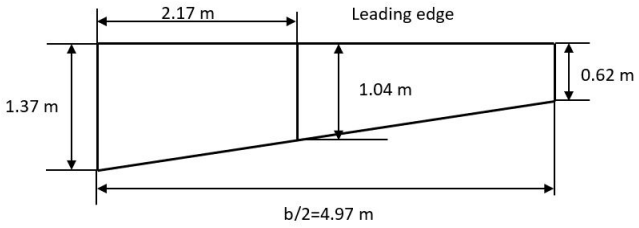

Figure 3: Wing Outline

3. Stress Analysis and Design

3.1 Spanwise lift distribution

The spanwise loading distribution is a critical aspect that concerns both aerodynamicists and stress analysts in the design and analysis of an aircraft. Aerodynamicists optimize the spanwise loading distribution to enhance aerodynamic performance, while stress analysts use this information to assess and reinforce the structural integrity of the aircraft. Balancing these considerations is essential in achieving an aircraft design that is both aerodynamically efficient and structurally sound. In this study, the Schrenk method [14] is employed among the numerous widely used approximate methods.

Schrenk method The Civil Aeronautics Administration (CAA) has approved Dr. Ing Oster Schrenk's approximate method as a satisfactory method to determine span-wise lift distribution in civil aircraft [14]. Schrenk method relies on the fact the the lift distribution does not differ much elliptical platform shape if:

- The wing is upswept.
- The wing has no aerodynamic twist.

The lift force distribution on wings can be estimated using this approximation method. By calculating the average lift per unit span between the planform lift distribution and the elliptical lift distribution, Schrenk methods approximate the force distribution [14]. This method's mathematical model is displayed below.

$$L_{\text{elliptical}} = \frac{4S}{\pi b}\sqrt{1 - \left(\frac{2y}{b}\right)^2} \tag{4}$$

$$L_{\text{planform}} = \frac{2S}{(1+\lambda)b}\left(1 + \frac{2y}{b}(\lambda - 1)\right) \tag{5}$$

$$L_{\text{schrenk}} = \frac{L_{\text{elliptical}} + L_{\text{planform}}}{2} \tag{6}$$

Based on the half wingspan, the wing loading calculations were made. The half wing span is discretized into 15 segments to calculate the lift as shown in Figure 4.

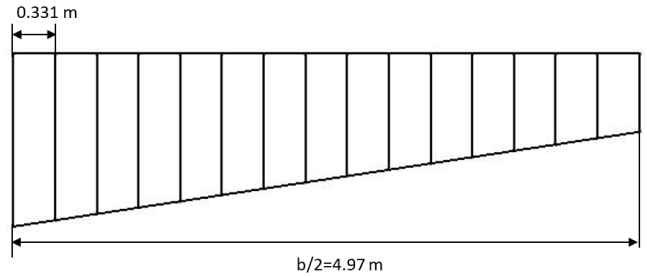

Figure 4: Wing span segments

The spanwise lift distribution of half wing span is shown in Figure 5.

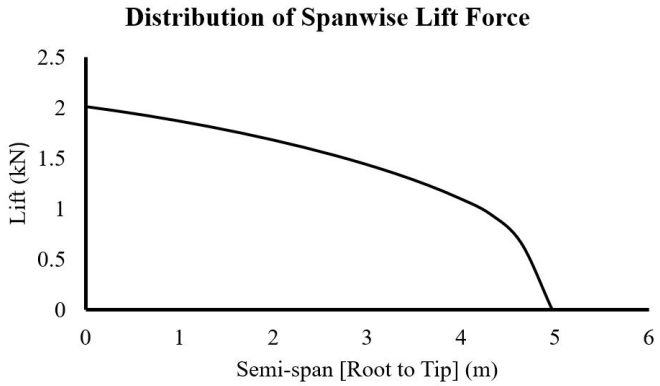

Figure 5: Spanwise lift force distribution based on Schrenk calculation

Values for Shear force and Bending moment are computed using a span-wise increment (Δy) as

$$\text{Shear force} = \int_0^{b/2} w \cdot dy = \sum_{i=1}^{i=n} \left(\frac{w_1 + w_2}{2} \right) \cdot \Delta y \qquad (7)$$

$$\text{Bending Moment} = \int_0^{b/2} S \cdot F \cdot dy = \sum_{i=1}^{i=n} \left(\frac{S \cdot F_1 + S \cdot F_2}{2} \right) \cdot \Delta y \quad (8)$$

The shear force distribution and bending moment distribution is shown in Figure 6.

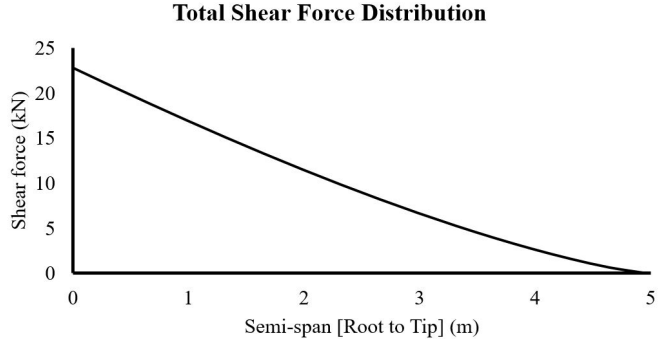

Figure 6: Shear force distribution

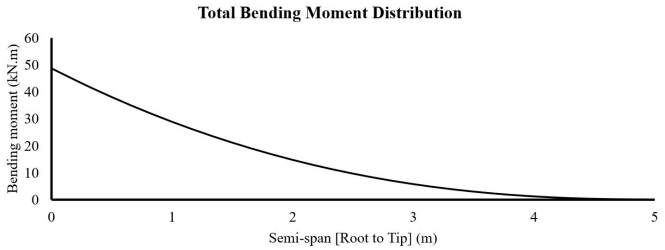

Figure 7: Bending moment distribution

For two spars wing model the position of the front spar is assumed at 25% of MAC and rear spar is assumed at 75% of MAC [15]. Lift force distribution: Lift force on front spar = Lift x (distance between Center of pressure and Rear spar/distance between Front spar and Rear spar) = 1204 N Lift force on rear spar = 803 N Lift force on front spar = 60 % of total lift force

Shear force and Bending moment are distributed in same ratio as that of the lift force.

3.2 Materials Properties

Two materials Steel alloy AISI 4340 and 2024-T351 aluminum alloy due to its high strength, slow crack growth rate as well as good fatigue life is selected for the study [16].

Table 1: AISI-4340 Material Properties

S/N	Properties	Value
1	Density (kg/m^3)	7833
2	Elastic modulus (MPa)	199948
3	Poisson's ratio	0.32
4	Tensile Ultimate Strength (MPa)	1792
5	Tensile Yield Strength (MPa)	1496

Table 2: Aluminum 2024-T351 Material Properties

S/N	Properties	Value
1	Density (kg/m^3)	2768
2	Elastic modulus (MPa)	73774
3	Poisson's ratio	0.33
4	Tensile Ultimate Strength (MPa)	427
5	Tensile Yield Strength (MPa)	317

3.3 Stress Analysis of Spar

According to the design and strength requirement, number of spar is determined for the wing. Two spars are considered for the study. The two spars shares the total lift load depending up on the center of lift. During spar analysis, the lift load calculated in section 3.1 is applied to the models at one end and the other end is fixed. The cross-section of I-spar is shown in Figure8.

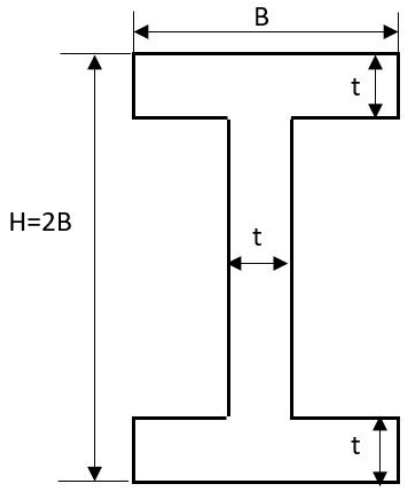

Figure 8: I-spar cross-section

Aluminium alloy Al2024-T351 is considered for analysis and results are tabulated in Table 3.

Table 3: Spar models with Al2024-T351 materials

Model description and results	Model 1	Model 2	Model 3
Spar height(H) (mm)	150	150	150
Spar width(B) (mm)	75	75	75
Flange thickness(t) (mm)	5	7.5	10
Web thickness(t) (mm)	5	7.5	10
Max. Von Mises Stress (MPa)	458.9	316	215.6
Deformation (mm)	403.2	283.3	223.4
Evaluation	U	S	S

*S=Satisfied, U=Unsatisfied

Model 2 and 3 satisfies the strength requirement of aluminium alloy. However, Model 3 is selected for wing-fuselage attachment lug analysis due to its lower stress and less displacement.

Steel alloy AISI4340 is considered for analysis and results are tabulated in Table 4.

Table 4: Spar models with AISI4340 materials

Model description and results	Model 4	Model 5	Model 6
Spar height(H) (mm)	150	150	150
Spar width(B) (mm)	75	75	75
Flange thickness(t) (mm)	5	7.5	10
Web thickness(t) (mm)	5	7.5	10
Max. Von Mises Stress (MPa)	457	315.4	215.4
Deformation (mm)	148.8	104.5	82.42
Evaluation	S	S	S

*S=Satisfied, U=Unsatisfied

Model 4,5 and 6 satisfies the strength requirement of steel alloy.However, Model 6 is selected for wing-fuselage attachment lug analysis.

3.4 Stress Analysis of Wing-Fuselage Attachment Lug

Figure 9 depicts the wing fuselage attachment lug that was taken into consideration for the study. [17] carried out the analysis on joints used in aircraft. The outcomes demonstrated that, in comparison to a straight joint, a tapered joint had provided good performance. Additionally, the lug is simple to assemble and can be manufactured effectively.

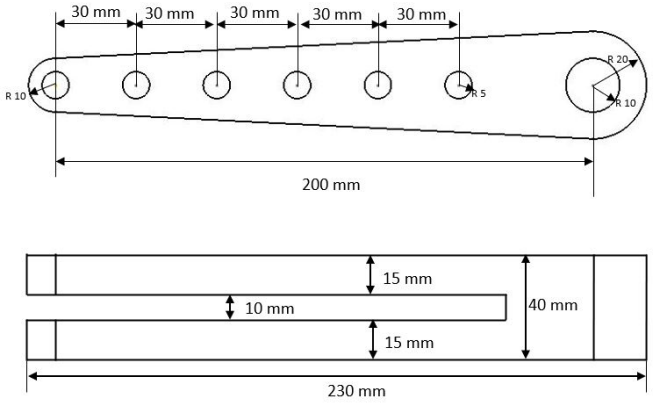

Figure 9: Dimensions of the wing-fuselage attachment lug

The attachment bracket is made up of a section of the spar and a lug that are fastened together with bolts. The lug consists of bolt holes which will be connected to the spar. In CATIA V5, the wing-fuselage attachment bracket and I-spar were modelled. Two cases of static stress analysis were performed for the wing fuselage attachment lug models.

Case 1: Analysis with Al2024-T351 and AISI4340 materials

In Case 1, Al2024-T351 material is considered for Spar and AISI4340 is considered for Lugs and Bolts. Table 5 describes two models with different lug thickness. Table 6 describes two models with different number of bolts.

Table 5: Case 1 wing-fuselage attachment models with different lug thickness

Model description and results	Model 1	Model 2
Spar height(H) (mm)	150	150
Spar width(B) (mm)	75	75
Flange thickness(t) (mm)	10	10
Web thickness(t) (mm)	10	10
Lug thickness(t) (mm)	30	40
No. of bolts	6	6
Max. Stress on Lug (MPa)	1531	1185
Max. Stress on I-spar bolt hole (MPa)	588.8	502.9
Deformation (mm)	3.208	2.758
Evaluation	U	U

From Table 5 it is observed that increasing lug thickness from 30 mm to 40 mm reduces stress on both the lug hole and spar bolt hole. However, the stress observed is higher than the yield stress of Al2024-T351 on spar bolt hole. Therefore the models in Table 5 do not satisfies the strength requirement.

From Table 6 it is observed that increasing number of bolts reduces stress on both the lug hole and spar bolt hole.And decreasing number of bolts increases stress on both the lug hole and spar bolt hole. However, the stress observed is higher than the yield stress of Al2024-T351 on spar bolt hole. Therefore the models in Table 6 do not satisfies the strength requirement.

Table 6: Case 1 wing-fuselage attachment models with different no. of bolts

Model description and results	Model 3	Model 4
Spar height(H) (mm)	150	150
Spar width(B) (mm)	75	75
Flange thickness(t) (mm)	10	10
Web thickness(t) (mm)	10	10
Lug thickness(t) (mm)	40	40
No. of bolts	7	5
Max. Stress on Lug (MPa)	1181	1190
Max. Stress on I-spar bolt hole (MPa)	469.8	559.3
Deformation (mm)	2.713	2.826
Evaluation	U	U

Case 2: Analysis with AISI4340 materials

In Case 2, AISI4340 materials is considered for Spar, Lug and Bolts.

Table 7: Case 2 wing-fuselage attachment models with different lug thickness

Model description and results	Model 5	Model 6
Spar height(H) (mm)	150	150
Spar width(B) (mm)	75	75
Flange thickness(t) (mm)	10	10
Web thickness(t) (mm)	10	10
Lug thickness(t) (mm)	30	40
No. of bolts	6	6
Max. Stress on Lug (MPa)	1457	1117
Max. Stress on I-spar bolt hole (MPa)	832.7	715.8
Deformation(mm)	2.165	1.8
Evaluation	S	S

From Table 7 it is observed that increasing lug thickness from 30mm to 4mm reduces stress on both the lug hole and spar bolt hole. The stress observed is less than the yield stress of AISI4340 on both lug hole and spar bolt hole. Therefore the models in Table 7 do satisfies the strength requirement.

Table 8: Case 2 wing-fuselage attachment models with different no. of bolts

Model description and results	Model 7	Model 8
Spar height(H) (mm)	150	150
Spar width(B) (mm)	75	75
Flange thickness(t) (mm)	10	10
Web thickness(t) (mm)	10	10
Lug thickness(t) (mm)	40	40
No. of bolts	5	4
Max. Stress on Lug (MPa)	1121	1131
Max. Stress on I-spar bolt hole (MPa)	784.7	900.2
Deformation (mm)	1.843	1.913
Evaluation	S	S

From Table 8 it is observed that increasing number of bolts reduces stress on both the lug hole and spar bolt hole. And decreasing number of bolts increases stress on both the lug hole and spar bolt hole. The stress observed is less than the yield stress of AISI4340 on both lug hole and spar bolt hole. Therefore the models in Table 8 do satisfies the strength requirement.

From the Table 7, Model 6 is selected for the designed aircraft because of low lug stress and spar bolt hole stress comparatively.

Figure 11 illustrates the loads and boundary conditions that are applied to the wing fuselage lug attachment bracket. 68003.73 N is the load applied at the bracket's root. It is introduced at one end of the spar beam in upward direction as maximum lift is generated in the wings during take-off. In essence, this load will produce the necessary bending moment at the bracket's root, where the fuselage and wings will be fastened. At the semicircular circumferential region, the top and bottom lug holes of the wing fuselage attachment bracket are constrained with all six degrees of freedom.

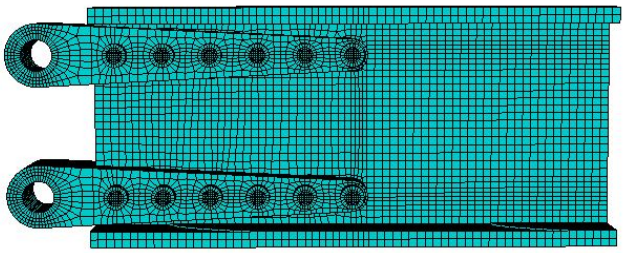

Figure 10: Meshed model of the wing-fuselage attachment

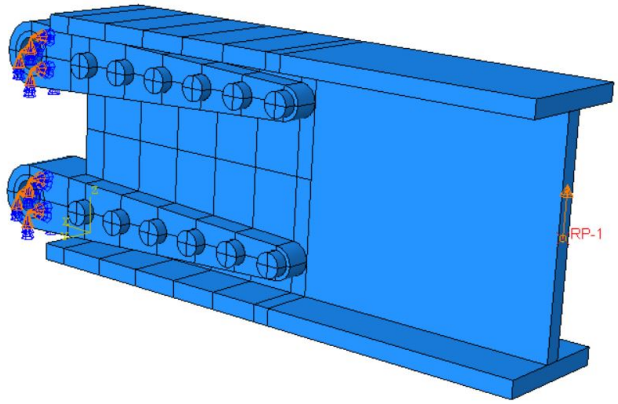

Figure 11: Load and Boundary Condition

Figure 12 displays the stress values at the lug hole. At the midpoint of the top lug hole, a maximum stress of 1117 N/mm^2 is noted.

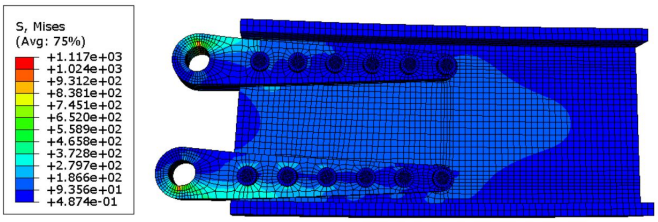

Figure 12: Maximum stress of wing fuselage attachment

The stress on spar bolt holes is observed is shown in figure 13. At bottom first hole, a maximum stress of 715.8 N/mm^2 is noted.

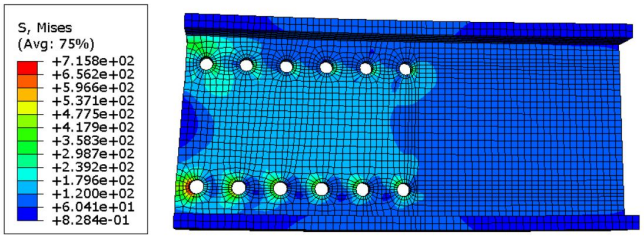

Figure 13: Maximum stress of wing fuselage attachment

The displacement contour in figure 14 shows a maximum displacement of 1.8 mm at the cantilever structure's free end.

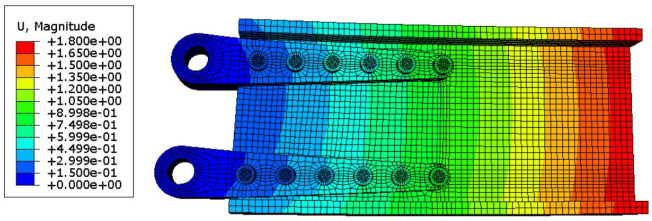

Figure 14: Maximum displacement of wing fuselage attachment

4. Results and Discussions

Case 1:
Finite element analysis was performed on the wing fuselage attachment models by assigning Aluminium alloy and Steel alloy as the engineering materials.Under static loading conditions, results were analysed for Von-Mises stress and total deformation. It is observed that increasing lug thickness from 30 mm to 40 mm reduces stress on both the lug hole and spar bolt hole. Also it is observed that increasing number of bolts reduces stress and decreasing number of bolts increases stress on both the lug hole and spar bolt hole respectively. For all four models, the stress observed is higher than the yield stress of Al2024-T351 on spar bolt hole. Therefore, we conclude that case 1 models do not satisfies the strength requirement.

Case 2:
Finite element analysis was performed on the wing fuselage attachment models by assigning Steel alloy as the engineering material. Under static loading conditions, results were analysed for Von-Mises stress and total deformation. It is observed that increasing lug thickness from 30 mm to 40 mm reduces stress on both the lug hole and spar bolt hole. Also it is observed that increasing number of bolts reduces stress and decreasing number of bolts increases stress on both the lug hole and spar bolt hole respectively. For all four models, the stress observed is less than the yield stress of AISI4340 on lug hole and spar bolt hole. Therefore, we conclude that case 2 models do satisfies the strength requirement.

From Case 2, Model 6 is selected as the wind fuselage attachment lug for the designed aircraft due to comparatively lower stress on both the lug hole and spar bolt hole.

5. Conclusion

This research paper has addressed the crucial aspects of designing and stress analysis of the wing-fuselage attachment for a general aviation aircraft.The finite element analysis of various attachment lug model is analyzed. From this study, following conclusions could be made:

- Maximum tensile stress is observed at top lug hole.
- Wing-fuselage attachment with combined materials fails to satisfy the strength requirement.
- Finite element analysis revealed that wing-fuselage attachment with AISI4340 materials only meets the strength requirement.
- Factor of safety for all the components of selected wing-fuselage attachment is more than 1; hence, designs are safe.

References

[1] A. Chinnamahammad Bhasha and Kulendran Balamurugan. Fracture analysis of fuselage wing joint developed by aerodynamic structural materials. *Materials Today: Proceedings*, 2020.

[2] R. Rigby and M.H. Aliabadi. Stress intensity factors for cracks at attachment lugs. *Engineering Failure Analysis*, 4(2):133–146, 1997.

[3] Seifert Dr Friedrich and Jaap Schijve. Fatigue crack growth of corner cracks in lug specimens. 1983.

[4] K. Kathiresan, H. S. Pearson, and G. J. Gilbert. Fatigue crack growth of a corner crack in an attachment lug. *International Journal of Fracture*, 22(2):R59–R63, Jun 1983.

[5] Harish E.R.M and Sartaj Patel. Stress analysis for wing attachment bracketof a six seater transport airframe structure. *International Journal of Innovative Research in Science, Engineering and Technology*, 2:3170–3177, 2013.

[6] A. Chinnamahammad bhasha and K. Balamurugan. Fracture analysis of fuselage wing joint developed by aerodynamic structural materials. *Materials Today: Proceedings*, 38:2555–2562, 2021. International Conference & Exposition on Mechanical, Material and Manufacturing Technology (ICE3MT).

[7] Praveenkumara B M. Stress analysis of fuselage segment with wing attachment bracket. Vol-40:1614–1619, 03 2020.

[8] Sri Bk. Stress analysis and fatigue life prediction of wing- fuselage lug joint attachment bracket of a transport aircraft. *International Journal of Research in Engineering and Technology*, 03:818–822, 05 2014.

[9] Gowtham Gajapathy, G. KUMAR, and AASA DARA. Design and optimization of lug bracket assembly. *INCAS BULLETIN*, 13:55–67, 03 2021.

[10] S. Gudmundsson. *General Aviation Aircraft Design: Applied Methods and Procedures*. Elsevier Science, 2021.

[11] DIAMOND DA-20 Eclipse - DV20 L1P L/G — doc8643.com. https://doc8643.com/aircraft/DV20. [Accessed 24-09-2023].

[12] Daniel Raymer. *Aircraft Design: A Conceptual Approach, Sixth Edition*. 09 2018.

[13] J. Roskam. *Airplane Design: Preliminary sizing of airplanes*. Airplane Design. Roskam Aviation and Engineering Corporation, 1989.

[14] O. Schrenk. A simple approximation method for obtaining the spanwise lift distribution. 08 1940.

[15] Feras Darwish, G.M. Atmeh, and Zeaid Hasan. Design analysis and modeling of a general aviation aircraft. 6:183–191, 04 2012.

[16] *MMPDS-14: Metallic Materials Properties Development and Standardization (MMPDS).. Chapters 1-9*. Federal Aviation Administration, 2019.

[17] Sravan Kumar, Siddharth Singh, Lokamanya Chikmath, and B. Dattaguru. Contact stress analysis and fatigue life estimates of aircraft structural joints. 12 2014.